Instrumented Impact Properties of Some Advanced Nuclear Reactor Pressure Vessel Steels

M.M. Ghoneim, A.M. Nasreldin, A.A. Elsayed, D. Pachur, and F.H. Hammad

Steels used to construct nuclear reactor pressure vessels are low-alloy ferritic steels. These steels should have good impact properties, i.e., low transition temperature and high upper shelf energy, both before and during service conditions. The most important service condition is the neutron irradiation. Extensive research and development was conducted to develop such steels. Instrumented impact testing was conducted on three advanced pressure vessel steels and, for comparison, a conventional pressure vessel steel. Both microstructures and fracture surfaces were examined using optical and scanning electron microscopic (SEM) techniques. In general, the advanced steels showed much better impact properties (lower ductile-brittle transition temperature and higher upper shelf energy) than the conventional steel. Load-time traces showed that increase in the fracture energy was mainly due to increase in the fracture propagation energy rather than the initiation energy. Improvement in the toughness level of the advanced steels compared to that of the HSST steel was related to the difference in chemical composition, microstructure, and fracture surface morphology.

Keywords
bainite microstructure, fractography, impact toughness, pressure vessel steels

1. Introduction

MORE THAN three quarters of the nuclear power stations all over the world already in operation or under construction use steel pressure vessels to house the reactor core. Successful and safe performance of the power stations depends on the reliability of steel pressure vessels (Ref 1). The ability of the reactor pressure vessel to resist brittle fracture is particularly important. This property depends on the material fracture toughness. In general, the steel fracture toughness decreases, and therefore the risk of brittle fracture can be considerably increased due to neutron irradiation during reactor operation. Charpy impact testing is used to determine the fracture toughness of pressure vessel steels. The two important parameters defined by this test are the ductile-brittle transition temperature (DBTT) and the upper shelf energy (USE). Irradiation shifts the DBTT to higher temperatures and lowers the USE. The magnitude of this effect (irradiation sensitivity) varies from one steel to another depending on several factors. The most important factor is chemical composition. Residual elements, especially copper (Cu) and phosphorus (P), increase irradiation embrittlement; Cu is the most serious residual element (Ref 2). The pressure vessel steel, therefore, must have (a) high initial fracture toughness (low DBTT and high USE), and (b) low irradiation sensitivity, mainly through minimizing the residual element content.

In addition, new designs of the nuclear pressure vessels use more forgings (Ref 3, 4), thereby minimizing welds and eliminating longitudinal welds, which facilitate in-service inspection. Furthermore, forging produces more uniform material, and the directionality of the mechanical properties is reduced compared to steel plates.

M.M. Ghoneim, A.M. Nasreldin, A.A. Elsayed, and **F.H. Hammad,** Atomic Energy Authority, Cairo, Egypt; and **D. Pachur,** KFA, Juelich, Germany.

2. Experimental

The present investigation used three steels representing the advanced pressure vessel steels and a reference steel representing the conventional pressure vessel steels (Ref 1). Advanced steels are a 20MnMoNi55 (ASTM A533-B C1.2) weld produced in Germany (GW), an ASTM A508 C1.3 forging produced in France (FF), and an ASTM A533-B C1.1 plate produced in Japan (JP). The conventional steel was an ASTM A533-B C1.1 plate (HSST 03 plate) produced in the USA (HSST), and it represents steels used in most nuclear reactor pressure vessels currently in operation. Chemical compositions and heat treatments are given in Tables 1 and 2.

Standard Charpy V-notch specimens 55 by 10 by 10 mm with 2 mm notch depth were machined from the four steels. The specimens were cut with their axis parallel to surface, perpendicular to rolling direction (plate), in tangential direction (forging), and with the notch perpendicular to surface. Impact testing was carried out according to ASTM E23 (Ref 5). An instrumented impact testing machine with a total energy of 300 J was used. Impact tests were conducted over a temperature range to generate full transition curves. The load-time traces produced from the test were utilized to obtain the dynamic yield strength and the fracture initiation and propagation energy. Optical micrographic observation was conducted by etching polished specimens using a solution of 4% picric acid and 1% nitric acid in methanol. Fracture surface morphology was examined using SEM.

3. Results

3.1 *Microstructure*

Microstructures of the investigated steels are presented in Fig. 1. The HSST and FF steels showed tempered bainitic structure. The JP steel showed a mixture of proeutectoid ferrite and bainite whereas the GW steel showed an acicular ferritic structure. The GW steel had the finest grain size, approximately 5 μm, whereas the FF steel had the coarsest grain size, approxi-

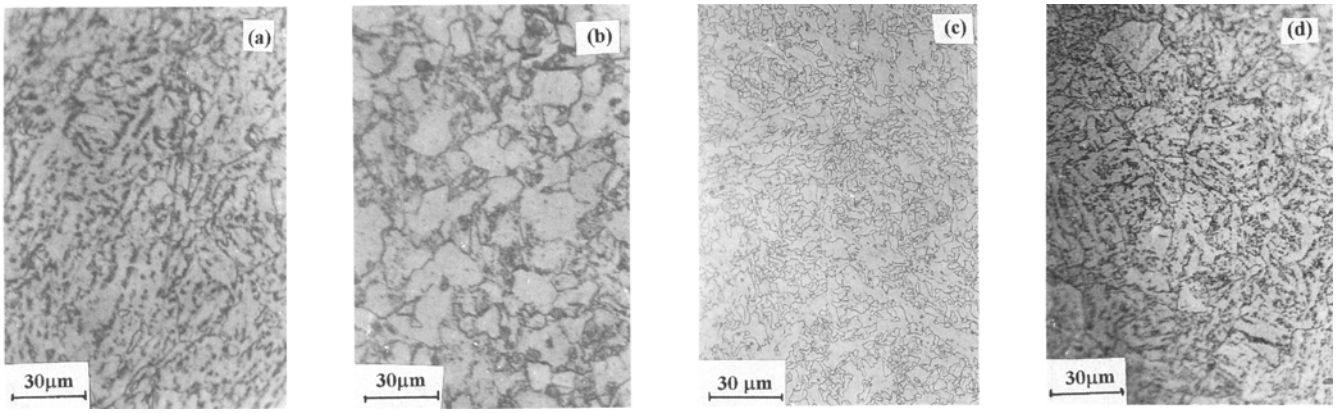

Fig. 1 Microstructures of tested steels: (a) FF (b) JP (c) GW and (d) HSST

Table 1 Chemical composition of pressure vessel steels

Element	Composition, wt %			
	GW	FF	JP	HSST
C	0.08	0.15	0.18	0.25
Si	0.17	0.28	0.22	0.25
Mn	1.45	1.3	1.4	1.33
Mo	0.61	0.5	0.58	0.51
Ni	0.93	0.7	0.66	0.65
Cr	0.02	0.24	0.2	0.1
P	0.011	0.009	0.007	0.011
Cu	0.035	0.07	0.015	0.13
S	0.006	0.007	0.004	0.018

Table 2 Heat treatment of pressure vessel steels

Steel	Heat treatment
GW	Postweld heat treat at 610 °C for 20 h; furnace cool
FF	Austenitize at 865 to 880 °C for 3 h; water quench; temper at 630 to 650 °C for 5.5 h; air cool; simulated postweld heat treat at 550 °C for 35 h and 615 °C for 16 h; furnace cool
JP	Austenitize at 880 °C for 8 h; water quench; temper at 660 °C for 6 h; air cool; simulated postweld heat treat at 620 °C for 26 h; furnace cool
HSST	At 915 °C for 12 h; air cool; austenitize at 860 °C for 12 h; water quench; temper at 635 °C for 12 h; furnace cool; simulated postweld heat treat at 610 °C for 40 h; furnace cool

mately 30 μm. The JP and HSST steels had grain sizes of 15 and 20 μm, respectively.

3.2 *Impact Properties*

Figure 2 shows the ductile-to-brittle transition curves of the tested steels. In general, the advanced steels show much better impact properties (lower DBTT and higher USE) than the conventional steel. Table 3 provides the DBTT at 41 J (T41J) and the USE values. The GW steel showed the lowest T41J (–73 °C) whereas the HSST steel had the highest value (6 °C). The advanced steels showed an USE of 183 to 200 J compared to 125 J for the HSST steel.

Table 3 Transition temperature and upper shelf energy

Steel	TT41J, °C	USE, J
GW	–73	183
JP	–44	196
FF	–57	200
HSST	6	125

Load-time curves for the tested steels were obtained at different temperatures. Figure 3 shows those representing specimens tested at room temperature. The GW and JP steels show upper shelf behavior. The FF steel was in the upper part of the transition region whereas the HSST steel was in the lower part of the transition region.

The load-time curves were utilized to obtain the dynamic yield strength (σ_{yd}), the fracture initiation energy (E_i), and propagation energy (E_p) as follows. The area under the load-time curve corresponds to the total energy absorbed energy. The energy up to the maximum load represents the fracture initiation energy, E_i, whereas the remainder represents the fracture propagation energy, E_p. The dynamic yield strength is calculated using the load at the yield point on the load-time curve (general yield load, P_{GY}) through the relationship (Ref 6):

$$\sigma_{yd} = (4P_{GY}W)/[1.274B(W - a)^2]$$

where B is the specimen thickness, W is the specimen width, and a is the notch depth.

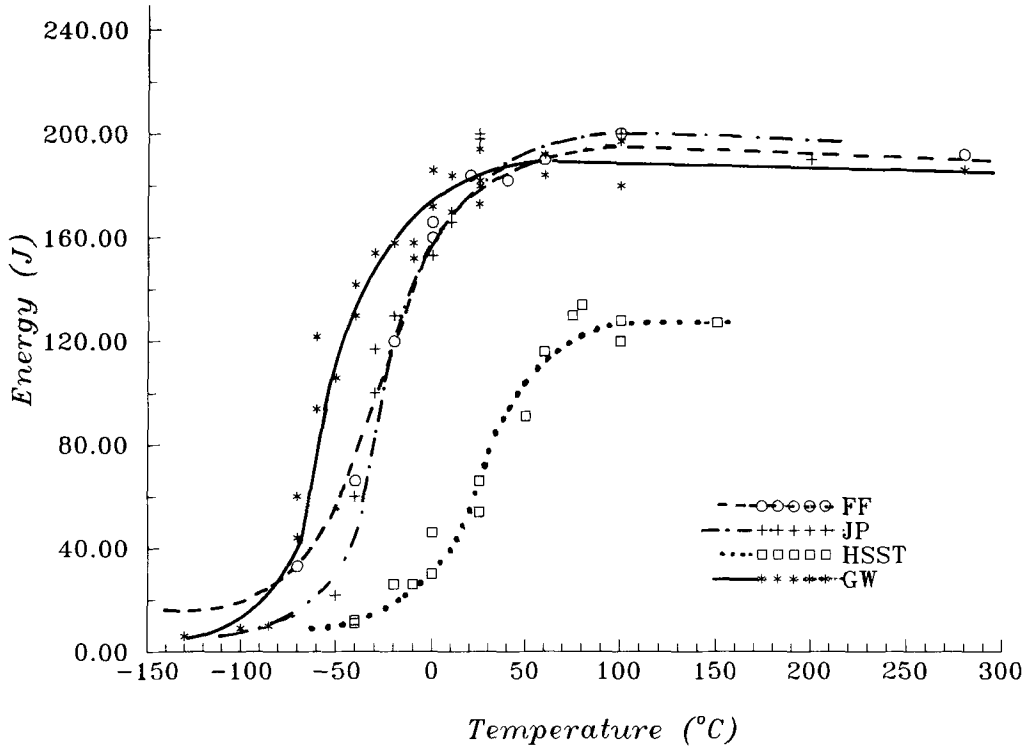

Fig. 2 Impact transition curves of tested steels

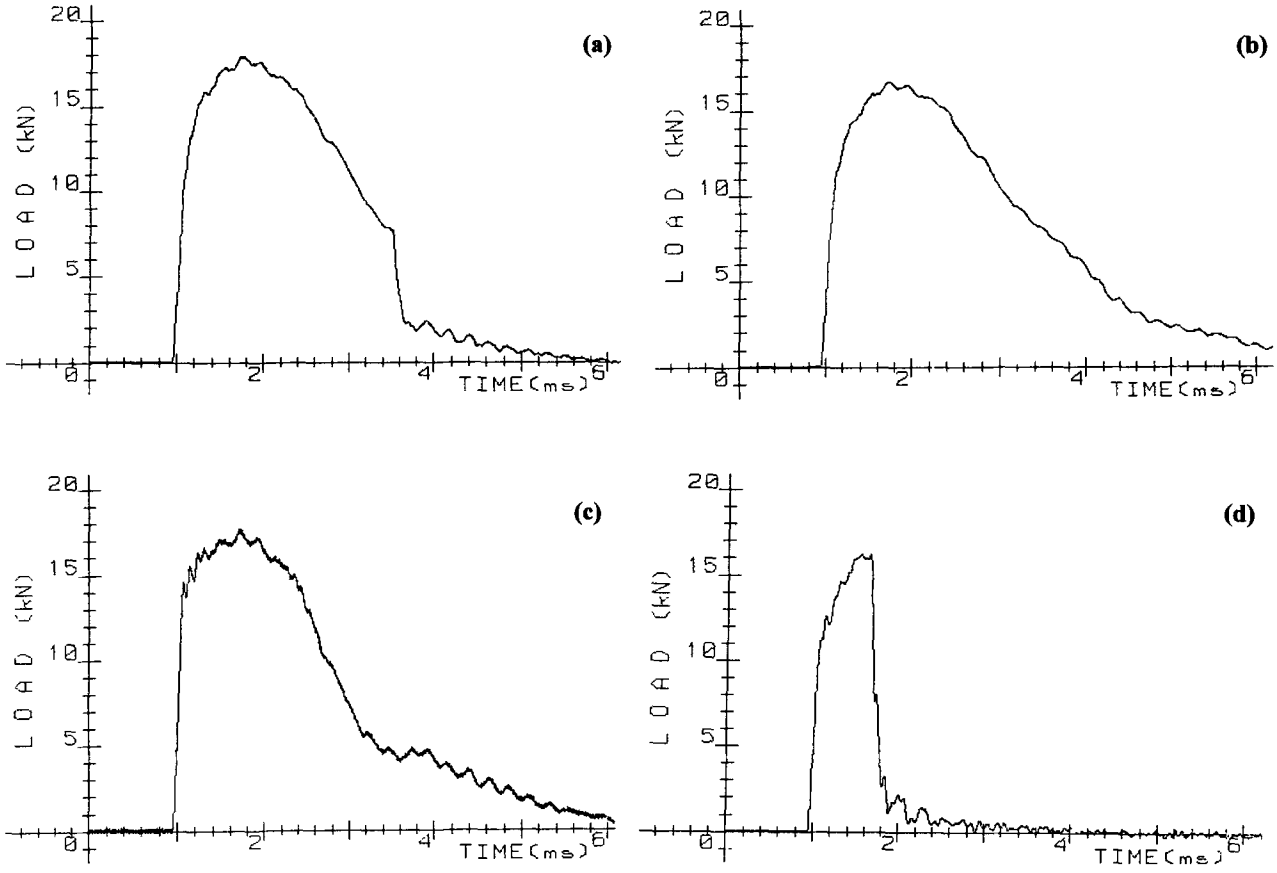

Fig. 3 Load-time curves of Charpy specimens tested at 25 °C: (a) FF (b) JP (c) GW (d) HSST

Figure 4 presents the σ_{yd} values with the testing temperature. The GW and FF steels show σ_{yd} values higher than those of the JP and HSST steels. Table 4 presents values of the dynamic yield strengths at room temperature together with the corresponding static values. The variation of E_i and E_p with test temperature is shown in Fig. 5 and 6, respectively. In the upper shelf region, the energy consumed during the crack propagation process, E_p, is much higher than that required for the crack initiation process, E_i. Table 5 gives values of E_i and E_p together with the total impact energy, E_t. E_i increased from 50 J for the reference steel (HSST) to 60 J for the advanced steels. At the same time, E_p exhibited a much greater increase, from 75 J for the HSST steel to approximately 130 J for the advanced steels. This indicates that the improvement in the USE for the advanced steels over that of the HSST steel was mainly due to the increase in the propagation energy fraction.

Another interesting observation is the decrease in E_i with increasing testing temperature in the upper shelf range. See Fig. 5.

3.3 *Fractography*

Fracture surface examination revealed that in the case of brittle fracture (lower shelf and transition regions) the fracture was by cleavage. In the ductile fracture case (transition and upper shelf regions), the fracture was by microvoid coalescence, and both large and small dimples were observed with no major

Table 4 Static (σ_y) and dynamic yield strength (σ_{yd}) at room temperature

Steel	σ_y, MPa	σ_{yd}, MPa
GW	517	666
JP	457	549
FF	532	637
HSST	474	578

Table 5 Values of initiation and propagation energy at upper shelf region

Steel	E_i, J	E_p, J	E_t, J
GE	60	123	183
JP	60	136	196
FF	62	138	200
HSST	50	75	125

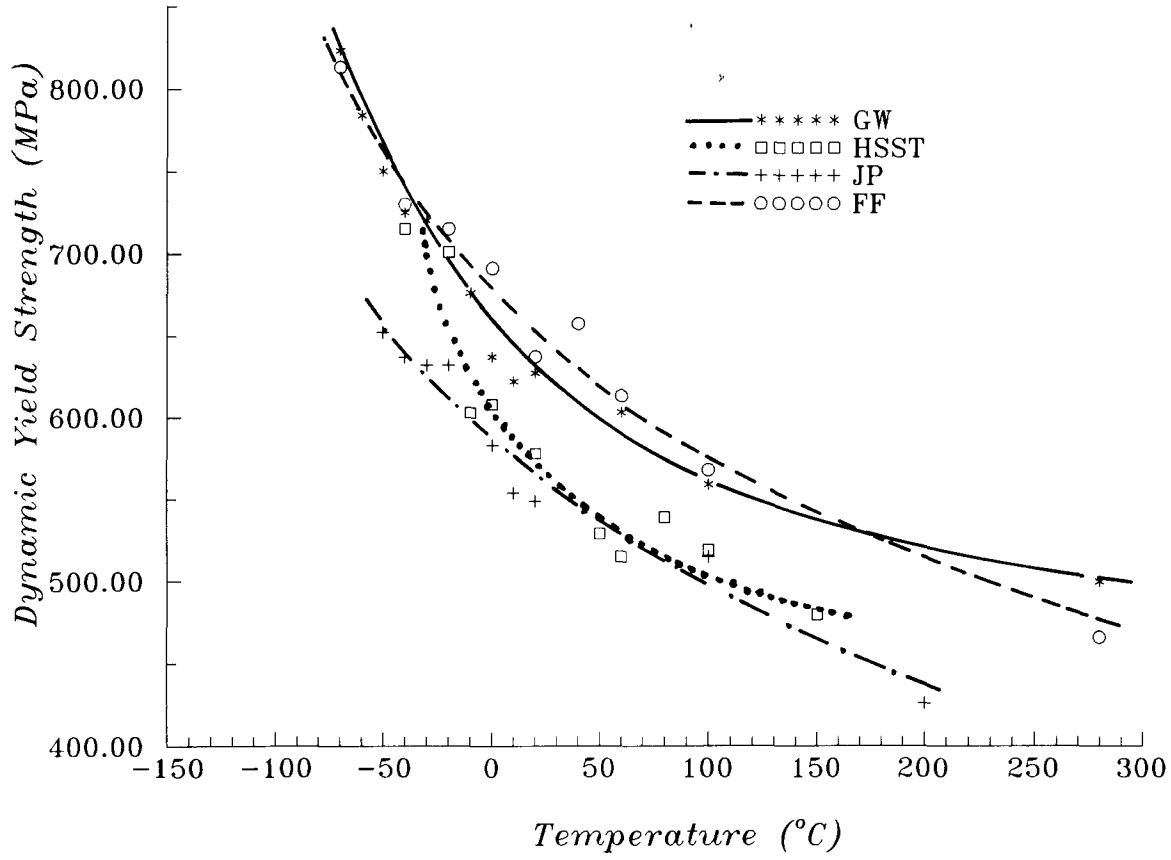

Fig. 4 Effect of test temperature on dynamic yield strength

differences among the four tested steels. Different cleavage fracture features for the different steels were found, as shown in Fig. 7.

The cleavage morphology in the HSST and JP steels comprised a facet-like arrangement with river patterns formed by cleavage lines and steps. The facet size is comparable to the grain size in both cases. The HSST steel showed continuous fracture plane, though orientation changed from grain to grain. However in the JP steel, the fracture plane experienced abrupt changes from one grain to the other.

In the FF and GW steels, the cleavage fracture was characterized by smaller cleavage facets connected by tear ridges (quasi-cleavage). The dimensions of the facets in the GW steel are comparable to the acicular ferrite grain size, which constitutes the microstructure of this steel. However, the facet size in the FF steel is probably related to a microstructural unit finer than the prior austenite grain size.

4. Discussion

Results show that the advanced steels exhibit better impact toughness than the reference steel (HSST steel) as expressed by their lower DBTT and higher USE values. See Table 3. In addition, advanced steels have higher strength in both static and dynamic conditions and have a good combination of strength and toughness compared to the HSST steel. This improvement in the toughness level can be considered along with the difference in chemical composition and microstructure between the four steels.

Advanced steels have relatively lower contents of carbon, sulfur, copper, and phosphorus compared to the HSST steel. Carbon (C) and sulfur (S) have detrimental effects on steel toughness. Increasing the C content raised the DBTT and decreased the USE (Ref 7). Increasing the S content also reduced the USE (Ref 8). C and S in steels form second phase particles (carbides and manganese sulfides). The particle density and/or size will increase with increasing C and S contents. Carbide particles participate in both cleavage and ductile dimple fracture. Crack initiation in cleavage fracture of steels occurs mostly at carbide particles. The increase in carbide density and/or size should lead to more crack nuclei, thereby decreasing the cleavage fracture strength and raising the DBTT (Ref 9).

When large and small second phase particles are present in steels, the ductile fracture process involves void nucleation and growth around large particles (MnS inclusions) and eventual coalescence via shear band localization from voids formed around the numerous smaller particles (carbides) (Ref 10). Increase in the density and/or size of the second phase particles, due to increasing S and C contents, should increase the density and/or size of both the large and small voids. This increase will enhance the premature termination of the void growth process and, consequently, reduce the fracture energy as shown in Fig. 2, 5, and 6.

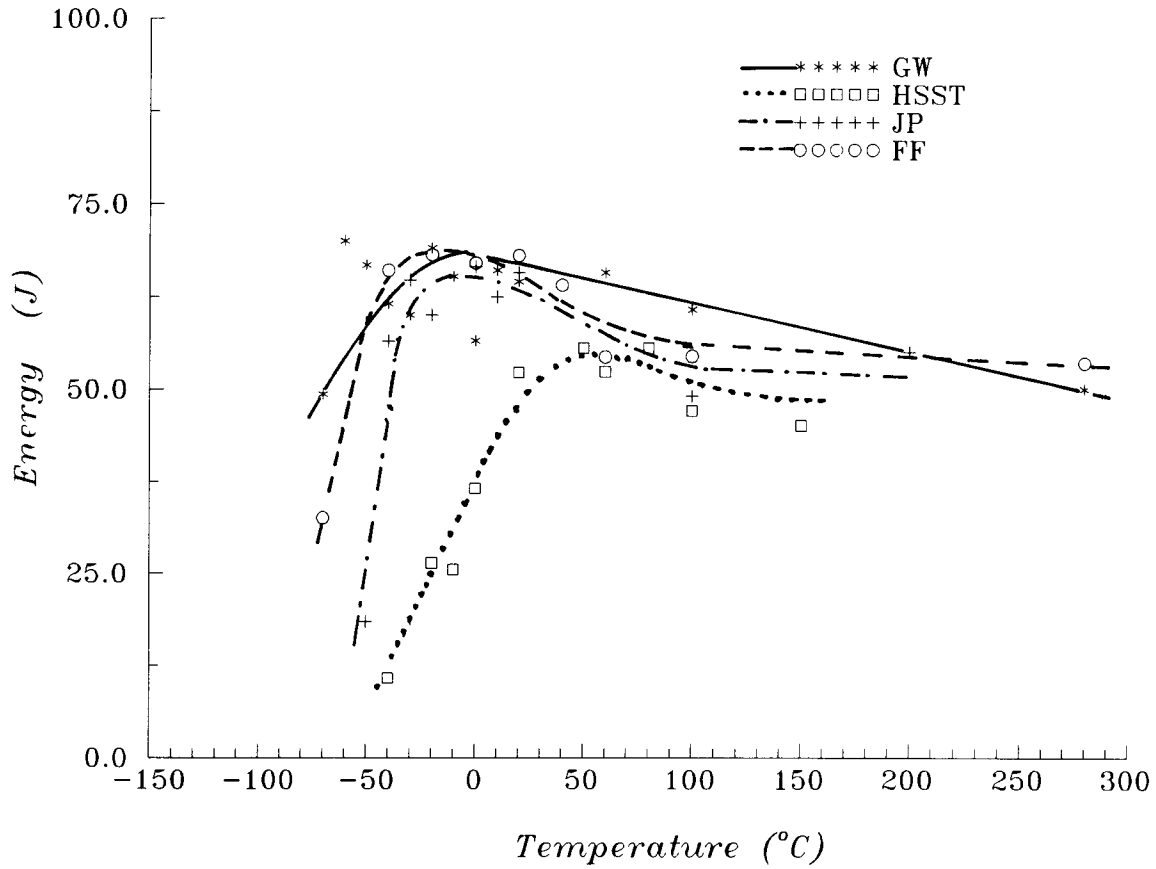

Fig. 5 Effect of test temperature on initiation energy

The microstructure also played a role in the toughness difference between the investigated steels. The different microstructures of these steels resulted in different features of cleavage fracture. While the HSST and the JP steels showed cleavage fracture appearance, the smaller facet size and the abrupt changes in the fracture path in the JP steel indicate a higher cleavage fracture strength. Such an improvement also accompanies the quasi-cleavage fracture features as those observed in the FF and GW steels. Microcracks in the advanced steels were hindered by more effective barriers than in the

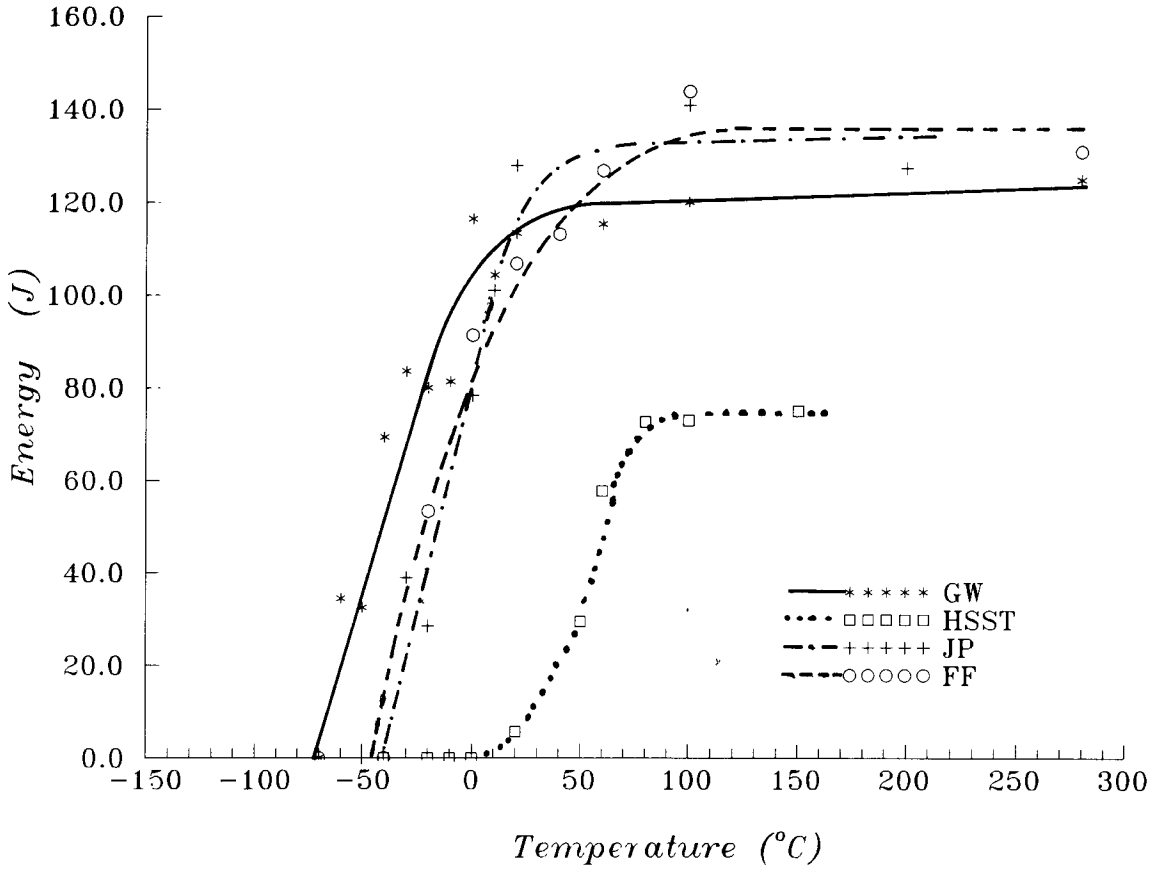

Fig. 6 Effect of test temperature on propagation energy

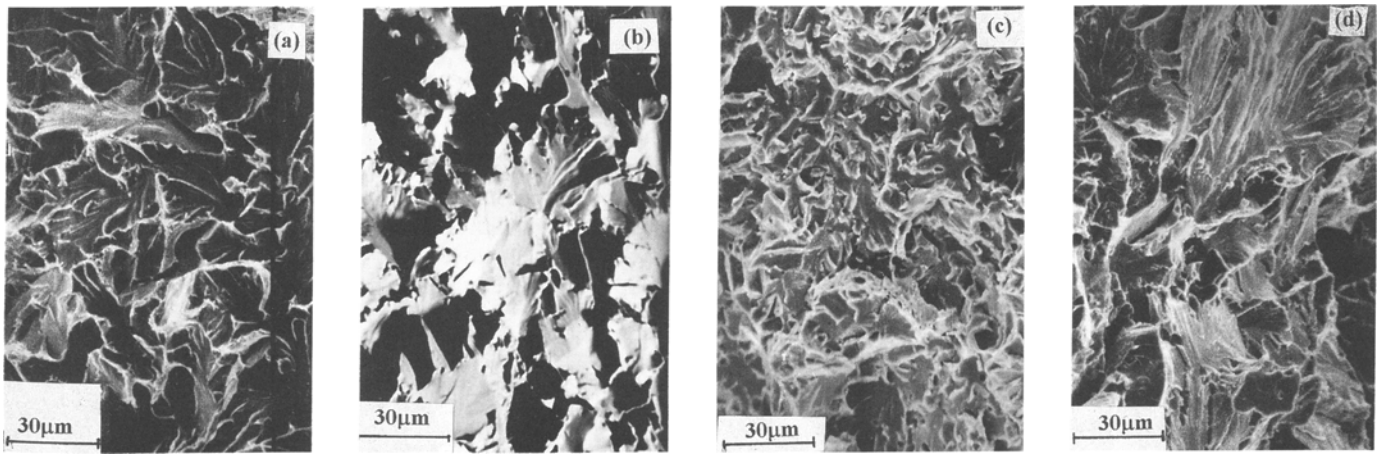

Fig. 7 Scanning electron fractographs of tested steels: (a) FF (b) JP (c) GW (d) HSST

HSST steel. Thus the crack is forced in reinitiate repeatedly. More energy is expended in the fracture process, thereby lowering the DBTT and increasing the fracture energy.

The difference in the impact energy between the advanced steels and the reference steel was mainly due to the difference in the fracture propagation energy. This result agrees with that of previous investigations (Ref 10, 11), which showed that the change in second-phase particle parameters (shape, volume, and distribution) has a much larger effect on the crack growth process than on the crack initiation process. This result was explained in the light the difference between the two processes (Ref 10). Initiation is fundamentally a two-dimensional process. In such a case, crack blunting takes place effectively in the straight ahead direction so that only those parameters associated with this direction will be important. Propagation, however, occurs by linkage of voids that are spatially distributed so that second-phase particle parameters of all three dimensions must be considered (Ref 10). The change in these parameters will affect the crack propagation process to a much higher degree than the crack initiation process.

The upper shelf of the Charpy impact energy curve is often viewed as a horizontal line; i.e., the USE does not vary with the test temperature. The present results showed that the energy fraction representing the fracture initiation, E_i, decreased with increasing test temperature. This result agrees with the typical behavior of plane-strain fracture toughness (K_{Ic} and J_{Ic}) with test temperature and is understandable because K_{Ic} and J_{Ic} are also concerned with the fracture initiation process.

5. Conclusions

Instrumented impact testing was carried out for three advanced pressure vessel steels in comparison with a conventional pressure vessel steel (HSST). The main conclusions are:

- Advanced steels acquire much better impact properties (lower ductile-brittle transition temperature and higher upper shelf energy) than the conventional steel.
- Increase in the impact energy of the advanced steels is mainly due to the increase in the fracture propagation energy rather than the fracture initiation energy.
- Improvement in the toughness of the advanced steels compared to that of the HSST steel is related to the difference in chemical composition and fracture surface morphology.
- Fracture initiation energy fraction of the impact energy decreases with increasing temperature in the upper shelf range, which agrees with the behavior of the fracture toughness K_{Ic}.

References

1. "Analysis of the Behaviour of Advanced Reactor Pressure Vessel Steels under Neutron Irradiation," IAEA Tech. Rep. 256, International Atomic Energy Agency, 1986
2. J.R. Hawthorne, in *Treatise on Materials Science and Technology*, Vol 25, C.L. Briant and S.K. Banerji, Ed., Academic Press, 1983, p 461-524
3. S. Kawaguchi, et al., *Nucl. Eng. Des.*, Vol 81, 1984, p 219-229
4. K. Kussmaul, *Nucl. Eng. Int.*, Dec. 1984, p 41-46
5. ASTM E23-72, *Annual Book of ASTM Standards*, Part 10 ASTM, 1980
6. W.L. Server, *J. Eng. Mater. Technol.*, Vol 100, 1978, p 183
7. T. Gladman and F. Pickering, in *Yield, Flow and Fracture of Polycrystals*, T.N. Baker, Ed., Applied Science Publishers, 1983, p 161
8. R.W. Hertzberg, *Deformation and Fracture Mechanics of Engineering Materials*, John Wiley & Sons, 1989, p 365
9. A.S. Tetelman and A.J. McEvily, *Fracture of Structural Materials*, John Wiley & Sons, 1967, p 268, 523
10. I.C. Howard and A.A. Willoughby, in *Developments in Fracture Mechanics-2*, G.G. Chell, Ed., Applied Science Publishers, 1983, p 39-99
11. R.O. Ritchie and A.W. Thompson, *Metall. Trans. A*, Vol 16, 1985, p 233-248